



## Peltier Cooling of Fermionic Quantum Gases

Ch. Grenier

*Institute for Quantum Electronics, ETH Zürich, 8093 Zürich, Switzerland*

A. Georges

*Collège de France, 11 place Marcelin Berthelot, 75005 Paris, France; Centre de Physique Théorique, Ecole Polytechnique, CNRS, 91128 Palaiseau Cedex, France; and DPMC, Université de Genève, CH-1211 Geneva, Switzerland*

C. Kollath

*HISKP, University of Bonn, Nussallee 14-16, D-53115 Bonn, Germany*

(Received 18 June 2014; revised manuscript received 6 August 2014; published 12 November 2014)

We propose a cooling scheme for fermionic quantum gases, based on the principles of the Peltier thermoelectric effect and energy filtering. The system to be cooled is connected to another harmonically trapped gas acting as a reservoir. The cooling is achieved by two simultaneous processes: (i) the system is evaporatively cooled, and (ii) cold fermions from deep below the Fermi surface of the reservoir are injected below the Fermi level of the system, in order to fill the “holes” in the energy distribution. This is achieved by a suitable energy dependence of the transmission coefficient connecting the system to the reservoir. The two processes can be viewed as simultaneous evaporative cooling of particles and holes. We show that both a significantly lower entropy per particle and faster cooling rate can be achieved in this way than by using only evaporative cooling.

DOI: 10.1103/PhysRevLett.113.200601

PACS numbers: 05.60.Gg, 05.30.Fk, 05.70.Ln, 67.85.Lm

**Introduction.**—The Peltier effect is a reversible thermoelectric phenomenon, in which heat is absorbed or produced at the junction of two materials forming a circuit in which a current is circulated [1]. Peltier cooling modules based on this effect are used for a variety of applications ranging from wine coolers to the cooling of electronic devices. The basic principle of a Peltier module is schematized in Fig. 1(c). It consists of two materials with Seebeck coefficients of opposite signs ( $p$ -type and  $n$ -type) arranged as indicated. A heat (entropy) current flows in both materials from the cold side to the hot side. Microscopically, this heat current corresponds to a flow of energetic electrons in the  $n$  branch: hot electrons above Fermi level are “evaporated” out of the cold plate. Similarly, a hole current flows in the same direction in the  $p$  branch, so that holes below Fermi level are being filled. Both processes lead to a rectification of the energy distribution of electrons in the cold plate [Fig. 1(b)] and, hence, to a decrease of its entropy.

In the context of mesoscopic electronic systems, thermoelectric effects as well as thermal properties and refrigeration have recently been the focus of renewed interest [2–4]. The cooling of low-dimensional nanostructures has been proposed [5–7] and experimentally realized [4,8,9], for example, by engineering a proper energy dependence of the transmission coefficients using quantum dots.

In the field of cold atomic Fermi gases, reaching lower temperatures is currently one of the most urgent challenges. Typically, the cooling of these gases is achieved using laser cooling followed by evaporative cooling [10,11]. Quantum degeneracy and very low absolute temperatures of the order

a few hundred nano-Kelvin are typically reached with these techniques, leading to the observation of many remarkable phenomena such as the BCS-BEC crossover [12]. However, the entropy per particle, which is the relevant quantity in these well isolated fermionic gases, is still too large ( $T/T_F \approx 0.1$ ) [13] to investigate many of the most intriguing quantum effects such as the Kondo effect [14,15],  $p$ -wave superfluidity [16–18], which shows a nontrivial topological feature [19] as the quantum Hall effect [20], low-temperature transport [21], spin liquids [22], or even antiferromagnetic order in the Hubbard model [23,24] [25].

Here, we propose an efficient cooling scheme for atomic Fermi gases which uses the Peltier effect in synergy with evaporative cooling. Our proposed setup is based on thermoelectric effects [26–35] and is displayed in Fig. 1(a). Two clouds of fermions, a reservoir  $R$  and a system  $S$  to be cooled, are prepared in harmonic traps. The initial Fermi energies of the two gases are  $E_{F,R(S)}^0 = \hbar\bar{\nu}(3N_{R(S)})^{1/3}$ , with  $\bar{\nu}$  the average trapping frequency [36] and  $N_R, N_S$  the atom numbers ( $N_R > N_S$ ). The lowest energy level of the reservoir is offset by  $\Delta\varepsilon \geq 0$  as compared to that of the system. Two processes are implemented in order to lower the entropy of the system. The first one is evaporative cooling at a rate  $\Gamma_{\text{ev}}(\varepsilon)$  applied to particles with energy higher than a threshold  $\varepsilon_1$ , chosen above the Fermi level  $E_{F,S}^0$ . The second simultaneous process is the injection of fermions from the reservoir into the system below the system’s Fermi level which can be viewed as an “evaporation” of holes.

This is achieved by connecting the traps by a constriction [37,38] characterized by an energy-dependent transmission

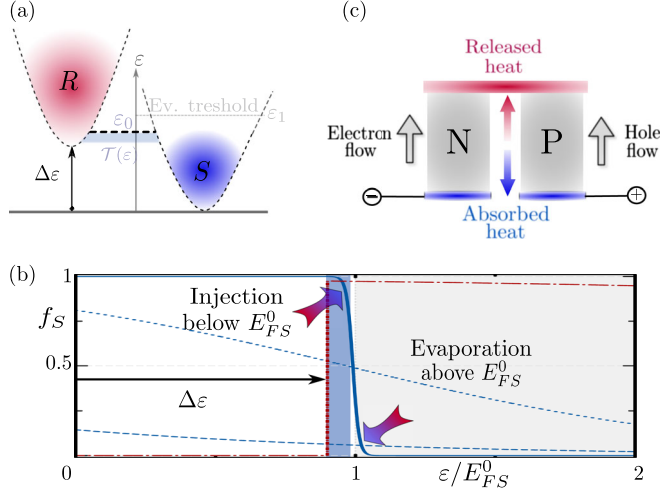


FIG. 1 (color online). (a) Sketch of the proposed Peltier cooling scheme: atoms are injected from deep energy levels of the reservoir cloud ( $R$ ) into the system cloud ( $S$ ) just below the Fermi level through a channel with an energy-dependent transmission  $\mathcal{T}(\epsilon)$ . Additionally, the system is submitted to evaporative cooling with a fixed evaporation threshold  $\epsilon_1$  above Fermi level, removing hot particles. (b) Evolution of the Fermi distribution of the system at three stages during the cooling process: initial (dashed blue curve,  $T_S \approx T_{FS}$ ), intermediate (dotted blue curve,  $T_S = 0.3T_{FS}$ ), and final (solid blue curve,  $T_S = 0.02T_{FS}$ ). The evolution, indicated by arrows, is calculated (see text) for  $\epsilon_1 = 1.05E_{FS}^0$ ,  $\gamma_{ev}\tau_0 = 15$ ,  $\epsilon_0 = 0.99E_{FS}^0$ ,  $\Delta\epsilon = 0.96E_{FS}^0$ , and  $E_{FS}^0 = 0.25E_{FR}^0$ . The blue and grey shaded regions indicate the injection and evaporation energy windows, respectively. The dashed-dotted curve is the final distribution of the reservoir. (c) Sketch of a Peltier cooling module. The  $n$ -like and  $p$ -like thermoelectric materials ensure the transport of low energy (electrons) and high energy (holes) particles, which, thus, carry heat from the cold (blue) to the hot (red) region.

$\mathcal{T}(\epsilon)$ . In an ideal setup, the transmission is chosen to have a boxlike dependence on energy: any state with energy above  $\Delta\epsilon$  and below a threshold  $\epsilon_0$  located just below the Fermi level of the system is perfectly transmitted [Fig. 1(a)].

The combination of these two processes, the evaporative cooling and the injection of fermions below the Fermi surface, induces an efficient cooling. This can be seen from the time evolution of the energy distribution displayed in Fig. 1(b). Starting initially from a broad hot distribution, it evolves towards a rectified distribution with a sharp drop at the Fermi level, characteristic of a low temperature. The parameters of the cooling process can be chosen, such that the atom number in the system changes only slightly, since the atom losses from evaporative cooling can be compensated by the injection of the reservoir atoms. At the same time, the reservoir is heated and loses atoms. However, the bottom of the energy distribution of the reservoir remains filled [Fig. 1(b)], ensuring an efficient injection of cool particles. The cooling process stops when the system energy distribution becomes equal to the reservoir distribution in the transmission window. We show below that both the final entropy per atom and the cooling rate are improved in comparison to evaporative cooling only, by approximately a factor of 4.

*Model of the cooling process.*—We describe the process in terms of coupled rate equations for the distribution functions  $f_S$  and  $f_R$ . We assume that thermalization in the system and in the reservoir is fast, so that they can be considered to be in thermodynamic equilibrium. Under this assumption, the particle current leaving the reservoir is given by the Landauer formula

$$I_N = \frac{1}{h} \int d\epsilon \mathcal{T}(\epsilon) [f_R(\epsilon) - f_S(\epsilon)] \\ = - \int d\epsilon g_R(\epsilon) \frac{df_R}{dt}(\epsilon) = \int d\epsilon g_S(\epsilon) \frac{df_S}{dt}(\epsilon).$$

In this expression,  $g_R(\epsilon) = (\epsilon - \Delta\epsilon)^2 / ((h\nu)^3) \vartheta(\epsilon - \Delta\epsilon)$  and  $g_S(\epsilon) = \epsilon^2 / ((h\nu)^3) \vartheta(\epsilon)$  are the density of states in the reservoir and in the system, with  $\vartheta$  the Heaviside function. The coupled evolution of the two distribution functions is, thus, given by

$$g_R(\epsilon) \frac{df_R(\epsilon)}{dt} = - \frac{\mathcal{T}(\epsilon)}{h} [f_R - f_S](\epsilon), \quad (1)$$

$$g_S(\epsilon) \frac{df_S(\epsilon)}{dt} = \frac{\mathcal{T}(\epsilon)}{h} [f_R - f_S](\epsilon) - \Gamma_{ev}(\epsilon) g_S(\epsilon) f_S(\epsilon). \quad (2)$$

In the second equation, the effect of evaporation has been included as a leak of high energy particles above a fixed energy threshold  $\epsilon_1$ , with an energy independent rate  $\Gamma_{ev}(\epsilon) = \gamma_{ev} \vartheta(\epsilon - \epsilon_1)$  [10]. Note that this differs from the usual definition of the evaporation rate as the rate of losses reducing the total particle number. Since  $\mathcal{T}(\epsilon)$  is dimensionless, the typical time scale that rules the time evolution in these equations is  $\tau_0 = hg_S(E_{FS}^0) = h(E_{FS}^0)^2 / ((h\nu)^3)$ . This is the compressibility divided by the “conductance” quantum, which has been identified as the time scale for the particle transport in previous experiments [26,37].

In principle the scattering of the atoms has to be taken into account in the evolution equations. However, since we assume the scattering to be the fastest time scale in the problem, we take it into account as an instantaneous rethermalization. This assumption is justified by a comparison of relevant time scales. A typical thermalization time found in experiments is around 100 ms (computed with the estimates given, e.g., in [39]). In contrast, the values for the transport times  $\tau_0$  are of the order of ten seconds (i.e., for 100 Hz average trapping frequency and  $E_F = 500$  nK in the reservoirs). Thus, the thermalization time is a small fraction of the transport time scales which ensures that the typical evolution by the transport is significantly slower than thermalization in the reservoirs, a regime which has already been observed experimentally [37,40].

The evolution of the system is implemented by time evolving Eqs. (1) and (2) for a time step  $\delta t = 0.1\tau_0$  which is small compared to the transport time and large compared to the thermalization time. The particle numbers  $N_{S,R}(t + \delta t)$  and energies  $E_{S,R}(t + \delta t)$  are computed and used to obtain the new values of the chemical potentials  $\mu_{S,R}$  and temperatures  $T_{S,R}$  assuming thermodynamic equilibrium for a

noninteracting gas. The resulting equilibrium Fermi functions  $f_S(t + \delta t, \varepsilon)$  and  $f_R(t + \delta t, \varepsilon)$  are subsequently evolved using the rate equations, and the entire procedure is repeated. This description of cooling is in line with the pulsed approach of evaporation developed, for example, in Refs. [10,41]. The time step  $\delta t$  is chosen small enough, such that it does not affect the resulting evolution.

Unless specified, a transmission of the form  $\mathcal{T}(\varepsilon) = \vartheta(\varepsilon_0 - \varepsilon)$  will be considered. This means that only states in the energy window  $\varepsilon \in [\Delta\varepsilon, \varepsilon_0]$  can be transmitted (“box-like” transmission). As was recently pointed out for electronic mesoscopic systems [7], and further discussed in the last section, this transmission is the optimal choice to achieve the best cooling performances. To summarize, the scheme involves three characteristic energy thresholds:  $\Delta\varepsilon \leq \varepsilon_0 \leq \varepsilon_1$ , corresponding, respectively, to the energy offset between  $R$  and  $S$ , the maximum injection energy into  $S$ , and the minimum evaporation energy out of  $S$ .

*Results and comparison to evaporative cooling.*—In the following, we demonstrate the potential of the proposed Peltier cooling scheme by comparing it to commonly used evaporative cooling. We focus on the reachable entropy per particle and on the cooling rate. The entropy per particle  $s$  in a trapped noninteracting Fermi gas is related to the ratio  $T/T_F$  by  $s = (\pi^2 k_B/2)(T/T_F)$  at low temperature, so that we use equivalently  $s$  or  $T/T_F$  below. The evolution of the entropy per particle is shown in Fig. 2(a). Assuming that the two gases are first prepared from a single cloud by evaporative cooling, we used a typically reached entropy per particle of  $T/T_F = 0.25$  as an initial value (with  $T_F$  the Fermi temperature of the total cloud). Initially, the ratio of the atom numbers between the system and the reservoir is chosen such that  $E_{FS}^0/E_{FR}^0 = N_S/N_R = 0.25$ , which leads to the initial entropy per atom of  $T_S/T_{FS} \approx 1.07$  and  $T_R/T_{FR} \approx 0.27$ . For the results in Fig. 2, we have chosen the evaporation threshold  $\varepsilon_1 = 1.05E_{FS}^0$ , the maximal transmission energy  $\varepsilon_0 = 0.99E_{FS}^0$ , i.e., close to the target Fermi energy (which is the initial one) and the chemical potential bias  $\Delta\varepsilon = 0.96E_{FS}^0$ . The rate  $\gamma_{ev}$  is chosen to be  $\gamma_{ev}\tau_0 = 15$ . Figure 2 shows that a very efficient reduction of the entropy per particle to a value of approximately  $T_S/T_{FS} \approx 0.02$  is achieved within a short time scale. At longer times, a slight rise in the entropy per particle sets in. The number of particles in the system initially has a very fast decay due to the dominating evaporation. However, the injection of electrons compensates this decrease at intermediate times, and an almost constant atom number close to the initial one is reached at long times.

In experimental setups, various heating mechanisms such as spontaneous emission [42], as well as particle losses, can drastically limit the lowest entropy that can be reached. The cooling process will stop being efficient when the cooling rate becomes comparable to the heating or emission rate, and therefore, it is important to compare these two rates. To this purpose, we define the cooling rate  $\eta$  as the time derivative of the entropy per particle:

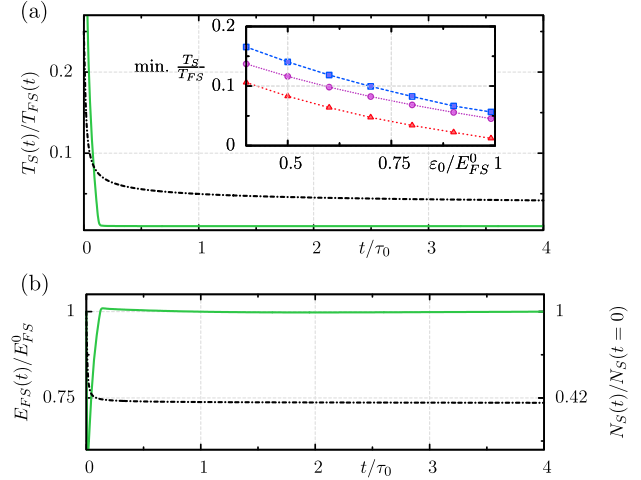


FIG. 2 (color online). Evolution during the cooling process of (a) the entropy per particle  $T_S(t)/T_{FS}(t)$  and (b) the Fermi energy  $E_{FS}(t)$  (left axis) and particle number  $N_S(t)$  (right axis). The solid curves are for the Peltier cooling with  $E_{FS}^0/E_{FR}^0 = 1/4$  and  $\varepsilon_1 = 1.05E_{FS}^0$ ,  $\gamma_{ev}\tau_0 = 15$ ,  $\varepsilon_0 = 0.99E_{FS}^0$ ,  $\Delta\varepsilon = 0.96E_{FS}^0$ . The dashed-dotted curves are for evaporative cooling only, with an initial particle number  $N = N_S + N_R$  and  $\varepsilon_1 = 1.05E_F$ . Inset: minimum entropy per particle achieved by Peltier cooling, as a function of  $\varepsilon_0$ , for:  $\varepsilon_1 = 1.05E_{FS}^0$  and  $(\varepsilon_0 - \Delta\varepsilon)/E_{FS}^0 = 3\%$  (red triangles), 20% (purple circles), and  $\varepsilon_1 = 1.5E_{FS}^0$ ,  $(\varepsilon_0 - \Delta\varepsilon)/E_{FS}^0 = 3\%$  (blue squares).

$\eta(t) = -(ds_S(t)/dt)$ , and display it in Fig. 3 versus the corresponding value of  $T_S(t)/T_{FS}(t)$ . The horizontal line stands for a typical value of the experimental heating rate. From this plot, one can directly read off the entropy per particle which can be reached (here about  $0.015T_S/T_{FS}$ ) in the presence of this heating rate.

To assess the usefulness of our cooling scheme, we compare it to evaporative cooling applied to the total initial cloud with  $N = N_R + N_S$  with the same initial temperature, here  $T/T_F = 0.25$ , and the same evaporation threshold relative to the Fermi energy  $\varepsilon_1 = 1.05E_F^0$ , where  $E_F^0$  is the initial Fermi energy of the total cloud. Since, for the evaporative cooling, no separation of the total cloud in two subclouds is performed, we use the index  $S$  to label the quantities of the entire cloud. We see, from Fig. 2, that at short times, the entropy reached by the proposed cooling scheme is much lower than the one reached by evaporative cooling. So, if one aims at reaching a given low value of  $T/T_F$ , this value is reached faster with the proposed scheme. At the same time, one sees that the particle number during the evaporative cooling is reducing drastically to about 40% of its initial value [44]. At infinite times, the evaporative cooling would empty the reservoir and, during this process, reach lower and lower entropy per particles. Nevertheless, as cooling takes place, evaporation is less and less efficient, and the cooling rate of evaporation slows down considerably: as seen in Fig. 3, the cooling rate for the Peltier scheme is much larger than for the evaporative scheme, at a given entropy per particle.

Because of this faster cooling rate, the temperatures which can be reached in the presence of heating or spontaneous emission are much deeper in the degenerate

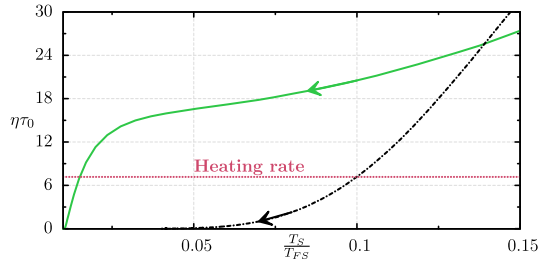


FIG. 3 (color online). Dimensionless cooling rate  $\eta(t)\tau_0$  as a function of  $T_S/T_{FS}$ , for the same parameters as in Fig. 2. The black dashed curve is for evaporative cooling only. Arrows indicate the direction of the time evolution. The horizontal (red) line indicates a typical heating rate (see, e.g., [43]) limiting these cooling processes.

regime when using the Peltier cooling. As seen in Fig. 3, for the chosen heating rate, an entropy per particle of order  $0.015T_S/T_{FS}$  is reached using the Peltier scheme, in contrast to  $0.10T_S/T_{FS}$  using evaporative cooling only.

The inset of Fig. 2(a) illustrates how the minimum of the entropy per particle depends on the parameters of the setup. The injection energy window  $\varepsilon_0 - \Delta\varepsilon$  should be relatively narrow to obtain a low entropy, but broad enough to allow for a fast cooling. Having, in addition, an evaporation threshold as close as possible to the target Fermi energy also improves the final value of the entropy per particle. The cooling scheme could be further optimized by changing some of the parameters in a time-dependent manner, as is commonly done for the threshold in evaporative cooling. For the sake of simplicity, we kept all parameters constant in our study.

*Possible implementations of the energy-dependent transmission.*—The Peltier cooling scheme relies on a transmission coefficient ensuring proper “energy filtering” between the two gases. We now discuss possible realizations of appropriate transmission functions which rely on state-of-the-art projection techniques [45–47]. The details of the two envisioned possibilities are discussed in the Supplemental Material [48]. We mainly consider two distinct forms [see Fig. 4(b)]. First, a narrow (delta-function-like) transmission in energy which can, for example, be realized by a single resonant level (or many in parallel) [54]. Such a narrow energy filter [55], has been predicted to achieve the maximization of the cooling efficiency or, equivalently, of the thermoelectric figure of merit. Second, an approximately boxlike transmission realized by two such resonant levels in series as discussed in the mesoscopic context [7,56]. Such a boxlike transmission with a finite width in energy is expected to show the maximum cooling power and best cooling rate (see Ref. [7] and the Supplemental Material [48]).

The results for the cooling rates as a function of  $T_S/T_{FS}$  are displayed in Fig. 4(a). As predicted, the idealized boxlike transmission (solid green line) allows for reaching a very low temperature with a fast cooling rate. Two quantum dots connected in series [blue dotted curve in Fig. 4(a)] realize a good approximation to the boxlike transmission and achieve a final entropy per particle which is only slightly higher. We also considered a single resonant level (red dashed-dotted

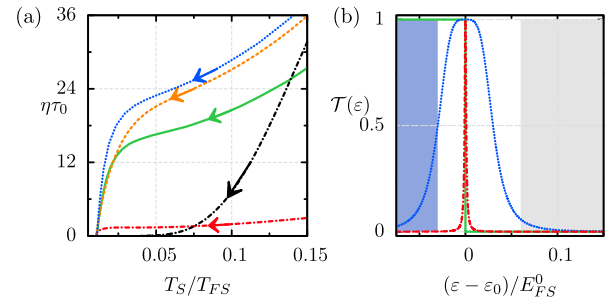


FIG. 4 (color online). (a) Dimensionless cooling rate  $\eta(t)\tau_0$  as a function of  $T_S/T_{FS}$ , for  $\Delta\varepsilon = 0.96E_{FS}^0$  and various transmissions centered at  $\varepsilon_0 = 0.99E_{FS}^0$  (the other parameters are taken as in Fig. 2): The (red) dotted-dashed and (orange) dashed curve correspond to a single and 100 parallel resonant level(s), respectively, with  $\Gamma = 1 \cdot 10^{-3}E_{FS}^0$ . The (blue) dotted curve is for two resonant levels in series of width  $\Gamma = 0.03E_{FS}^0$  and the (green) solid curve is for an ideal box transmission. The (black) dashed-dotted curve shows the evaporative cooling only. (b) The corresponding energy-dependent transmission coefficients. The grey area indicates states above  $\varepsilon_1$ , while the blue one indicates those below  $\Delta\varepsilon$ , which do not participate in transport.

curve), with a width such that a low final entropy comparable to that of the idealized box is achieved. In contrast to the latter, this leads to a much slower cooling rate [57]. This low cooling rate can, to some extent, be overcome by using many resonant levels in parallel (orange dashed curve): a fast initial cooling is then observed, comparable to that of the idealized box. In summary, we have identified two different ways of realizing efficient cooling, either by connecting relatively broad resonant levels in series, or by using a large number of narrow resonant levels in parallel. The attainable values of  $T_S/T_{FS}$  remain, in all considered cases, significantly better than what can be achieved from evaporation only.

*Conclusion.*—In this Letter, we have introduced a Peltier cooling scheme for fermionic gases, which combines conventional evaporation with energy-selective injection of particles. In a nutshell, this scheme can be described as a simultaneous evaporative cooling of particles and holes. We have proposed different realizations of the proper energy filtering between the reservoir and the cooled system, in line with the recent development of mesoscopic-like channels in cold atom gases [37,58]. The proposed scheme achieves fast and efficient cooling down to temperatures deep in the quantum degenerate regime, a much desired current goal in the field of atomic fermion gases. The present work also demonstrates that the recent fundamental studies of coupled particle and entropy transport in cold atomic gases [26–35] may also have useful implications for further experimental developments in the field.

We thank J.-P. Brantut, M. Büttiker, T. Esslinger, S. Krinner, H. Moritz, D. Papoular, J. L. Pichard, B. Sothmann, S. Stringari, and R. S. Whitney for useful discussions and suggestions. Support was provided by the Defense Advanced Research Projects Agency/Multidisciplinary University Research Initiatives-Optical Lattice Emulator

program, National centers of competence in research for Quantum Information Science and Technology of the Swiss National Science foundation, and the seventh framework program Project Thermiq.

- [1] H. J. Goldsmid, *Introduction to Thermoelectricity*, Springer Series in Materials Science (Springer, Dordrecht, 2009).
- [2] O. Entin-Wohlman, Y. Imry, and A. Aharony, *Phys. Rev. B* **82**, 115314 (2010).
- [3] R. Sánchez and M. Büttiker, *Phys. Rev. B* **83**, 085428 (2011).
- [4] F. Giazotto, T. T. Heikkilä, A. Luukanen, A. M. Savin, and J. P. Pekola, *Rev. Mod. Phys.* **78**, 217 (2006).
- [5] H. L. Edwards, Q. Niu, and A. L. de Lozanne, *Appl. Phys. Lett.* **63**, 1815 (1993).
- [6] A. N. Jordan, B. Sothmann, R. Sánchez, and M. Büttiker, *Phys. Rev. B* **87**, 075312 (2013).
- [7] R. S. Whitney, *Phys. Rev. Lett.* **112**, 130601 (2014).
- [8] J. R. Prance, C. G. Smith, J. P. Griffiths, S. J. Chorley, D. Anderson, G. A. C. Jones, I. Farrer, and D. A. Ritchie, *Phys. Rev. Lett.* **102**, 146602 (2009).
- [9] A. V. Timofeev, M. Helle, M. Meschke, M. Möttönen, and J. P. Pekola, *Phys. Rev. Lett.* **102**, 200801 (2009).
- [10] W. Ketterle and N. van Druten, *Adv. At. Mol. Opt. Phys.* **37**, 181 (1996).
- [11] C. J. Pethick and H. Smith, *Bose-Einstein Condensation in Dilute Gases*, 2nd ed. (Cambridge University Press, Cambridge, England, 2008).
- [12] W. Ketterle and M. Zwierlein, *Making, Probing and Understanding Ultracold Fermi Gases*, Rivista del Nuovo Cimento Vol. 31 (Società Italiana di Fisica, Bologna, 2008).
- [13] D. C. McKay and B. DeMarco, *Rep. Prog. Phys.* **74**, 054401 (2011).
- [14] J. Bauer, C. Salomon, and E. Demler, *Phys. Rev. Lett.* **111**, 215304 (2013).
- [15] A. C. Hewson, *The Kondo Problem to Heavy Fermions* (Cambridge University Press, Cambridge, England, 1993).
- [16] V. Gurarie, L. Radzihovsky, and A. V. Andreev, *Phys. Rev. Lett.* **94**, 230403 (2005).
- [17] Y. Ohashi, *Phys. Rev. Lett.* **94**, 050403 (2005).
- [18] C.-H. Cheng and S.-K. Yip, *Phys. Rev. Lett.* **95**, 070404 (2005).
- [19] N. Read and D. Green, *Phys. Rev. B* **61**, 10267 (2000).
- [20] N. Cooper, *Adv. Phys.* **57**, 539 (2008).
- [21] Y. Nazarov and Y. Blanter, *Quantum Transport: Introduction to Nanoscience* (Cambridge University Press, Cambridge, England, 2009).
- [22] M. Lewenstein, A. Sanpera, and V. Ahufinger, *Ultracold Atoms in Optical Lattices: Simulating Quantum Many-Body Systems* (Oxford University Press, Oxford, England, 2012).
- [23] R. Jördens, L. Tarruell, D. Greif, T. Uehlinger, N. Strohmaier, H. Moritz, T. Esslinger, L. De Leo, C. Kollath, A. Georges, V. Scarola, L. Pollet, E. Burovski, E. Kozik, and M. Troyer, *Phys. Rev. Lett.* **104**, 180401 (2010).
- [24] I. Bloch, J. Dalibard, and W. Zwerger, *Rev. Mod. Phys.* **80**, 885 (2008).
- [25] The entropy in the optical lattice depends strongly on the loading procedure, and heating might be induced by the scattering of the lattice light with an atom [13].
- [26] J.-P. Brantut, C. Grenier, J. Meineke, D. Stadler, S. Krinner, C. Kollath, T. Esslinger, and A. Georges, *Science* **342**, 713 (2013).
- [27] C. Grenier, C. Kollath, and A. Georges, [arXiv:1209.3942](https://arxiv.org/abs/1209.3942).
- [28] E. L. Hazlett, L.-C. Ha, and C. Chin, [arXiv:1306.4018](https://arxiv.org/abs/1306.4018).
- [29] A. Rancon, C. Chin, and K. Levin, [arXiv:1311.0769](https://arxiv.org/abs/1311.0769).
- [30] D. J. Papoular, G. Ferrari, L. P. Pitaevskii, and S. Stringari, *Phys. Rev. Lett.* **109**, 084501 (2012).
- [31] D. J. Papoular, L. P. Pitaevskii, and S. Stringari, [arXiv:1405.6026](https://arxiv.org/abs/1405.6026) [*Phys. Rev. Lett.* (to be published)].
- [32] L. A. Sidorenkov, M. K. Tey, R. Grimm, Y.-H. Hou, L. Pitaevskii, and S. Stringari, *Nature (London)* **498**, 78 (2013).
- [33] H. Kim and D. A. Huse, *Phys. Rev. A* **86**, 053607 (2012).
- [34] C. H. Wong, H. T. C. Stoof, and R. A. Duine, *Phys. Rev. A* **85**, 063613 (2012).
- [35] T. Karpiuk, B. Grémaud, C. Miniatura, and M. Gajda, *Phys. Rev. A* **86**, 033619 (2012).
- [36] The trap frequencies are chosen to be identical for simplicity even though their shape could be used for further optimization of the scheme.
- [37] J.-P. Brantut, J. Meineke, D. Stadler, S. Krinner, and T. Esslinger, *Science* **337**, 1069 (2012).
- [38] M. Bruderer and W. Belzig, *Phys. Rev. A* **85**, 013623 (2012).
- [39] J. Walraven, in *Quantum Dynamics of Simple Systems: Proceedings of the Forty Fourth Scottish Universities Summer School in Physics, Stirling, August 1994* (Taylor & Francis, London, 1997).
- [40] S. Krinner, D. Stadler, D. Husmann, J.-P. Brantut, and T. Esslinger, [arXiv:1404.6400](https://arxiv.org/abs/1404.6400).
- [41] K. Davis, M.-O. Mewes, and W. Ketterle, *Appl. Phys. B* **60**, 155 (1995).
- [42] C. J. Foot, *Atomic Physics*, Oxford Master Series in Atomic, Optical and Laser Physics, 1st ed. (Oxford University Press, New York, 2005).
- [43] R. Grimm, M. Weidemüller, and Y. B. Ovchinnikov, *Adv. At. Mol. Opt. Phys.* **42**, 95 (2000).
- [44] However, note that this value is still larger than the particle number in the system gas.
- [45] B. Zimmermann, T. Müller, J. Meineke, T. Esslinger, and H. Moritz, *New J. Phys.* **13**, 043007 (2011).
- [46] W. S. Bakr, J. I. Gillen, A. Peng, S. Fölling, and M. Greiner, *Nature (London)* **462**, 74 (2009).
- [47] J. F. Sherson, C. Weitenberg, M. Endres, M. Cheneau, I. Bloch, and S. Kuhr, *Nature (London)* **467**, 68 (2010).
- [48] See Supplemental Material at <http://link.aps.org/supplemental/10.1103/PhysRevLett.113.200601> for the discussion of possible experimental realizations, which includes [49–53].
- [49] D. S. Fisher and P. A. Lee, *Phys. Rev. B* **23**, 6851 (1981).
- [50] D. Stadler, S. Krinner, J. Meineke, J.-P. Brantut, and T. Esslinger, *Nature (London)* **491**, 736 (2012).
- [51] S. Krinner, D. Stadler, J. Meineke, J.-P. Brantut, and T. Esslinger, *Phys. Rev. Lett.* **110**, 100601 (2013).
- [52] J. Meineke, Ph.D. thesis, ETH Zürich 2012.
- [53] T. Müller, Ph.D. thesis, ETH Zürich 2011.
- [54] S. Datta, *Electronic Transport in Mesoscopic Systems*, Cambridge Studies in Semiconductor Physics and Microelectronic Engineering Vol. 3 (Cambridge University Press, Cambridge, England, 1997).
- [55] G. D. Mahan and J. O. Sofo, *Proc. Natl. Acad. Sci. U.S.A.* **93**, 7436 (1996).
- [56] K. H. Thomas and C. Flindt, *Phys. Rev. B* **89**, 245420 (2014).
- [57] The lowest entropy per particle which can be reached for the single resonant level is mainly determined by its width  $\Gamma$  and can be decreased considerably by lowering its width at the cost of slowing down its rate.
- [58] J. H. Thywissen, R. M. Westervelt, and M. Prentiss, *Phys. Rev. Lett.* **83**, 3762 (1999).